THE BALTIC JOURNAL
OF ROAD AND BRIDGE ENGINEERING

ISSN 1822-427X / eISSN 1822-4288
2016 Volume 11(1): 22–34

EVALUATION OF CALCULATION METHODS USED FOR ESTIMATING THE ULTIMATE MOMENT RESISTANCE OF BRIDGE DECKS REINFORCED WITH FRP BARS

Tomas Skuturna[1]✉, **Juozas Valivonis**[2]

Dept of Reinforced Concrete and Masonry Structures, Vilnius Gediminas Technical University, Saulėtekio al. 11, LT–10223 Vilnius, Lithuania
E-mails: [1]tomas.skuturna@vgtu.lt; [2]juozas.valivonis@vgtu.lt

Abstract. A statistical research of the calculation methods for calculating ultimate moments of concrete elements reinforced with fibre-reinforced plastic is presented. For this purpose a database of experimental results has been collected. Calculations of the ultimate moment resistance were performed according to three design recommendations. Wilk-Shapiro test were used to determine the distribution of experimental and theoretical data. The statistical research to evaluate the calculation methods was performed by testing the statistical hypothesis on the differences between theoretical and experimental values. It is suggested to calculate the coefficient of confidence for assessing the accuracy of calculation methods.

Keywords: concrete bridge deck, design methods, FRP bar reinforcement, statistical analysis.

1. Introduction

Concrete reinforced with steel bars is widely applied in modern construction. Corrosion of steel reinforcement in reinforced concrete structures in aggressive environments, however, causes serious problems during the service time of the constructions. Due to steel reinforcement corrosion, the service time of concrete constructions such as bridges shortens and the maintenance costs increase. Concrete bridge decks deteriorate more and faster than the other parts due to direct impact of the environment, moisture, freeze thaw cycles, de-icing salts, increasing traffic loads.

In order to avoid the problems caused by the corrosion, concrete constructions reinforced with steel reinforcement should be additionally protected from the factors causing corrosion or constructions can be reinforced with non-corroding reinforcement. As an alternative to steel reinforcement, FRP (fibre-reinforced plastic) reinforcement can be used (Bouguerra *et al.* 2011; Dang *et al.* 2014; Hassan *et al.* 2000; Matta, Nanni 2009).

Numerous studies on application and use of fibre reinforced polymers (FRP) in construction elements have been conducted. Additionally to reinforcement bars, wires and ropes, FRP can be used in the form of strips, sheets and lamellas. FRP reinforcement can also be applied not only for reinforcing new concrete constructions as internal reinforcement, it can also be used in strengthening the structures as external reinforcement (Aktas, Sumer 2014; Barris *et al.* 2012; Benzaid, Mesbah 2014; Daugevičius *et al.* 2012; Fayyadh, Razak 2014; Lale Arefi *et al.* 2014; Lapko, Urbanski 2015; Marčiukaitis *et al.* 2007; Meisami *et al.* 2013; Mostofinejad, Ilia 2014; Mostofinejad, Moghaddas 2014; Nelson, Fam 2014; Pakrastinsh *et al.* 2006; Serdjuks *et al.* 2003; Skuturna, Valivonis 2014a; Sprince *et al.* 2013; Sundarraja, Prabhu 2013; Szolomicki *et al.* 2015; Valivonis *et al.* 2014). FRP reinforcement, as compared to steel, is lighter, resistant to corrosion, has a higher tensile strength, and is transparent to magnetic fields and electrically non-conductive. FRP reinforcement bars are made from glass, aramid and carbon fibres are connected with epoxy resin, polyester and vinyl-ester. New generation FRP reinforcement in some countries is certified and meets the set standards. FRP reinforcement bars allow for handling the problems caused by reinforcement corrosion.

A bridge deck forms the driving surface and performs as a structural bending element. If FRP reinforcement bars are used in bridge decks, their service time, resistance to aggressive environment increase and the maintenance costs decrease. Published design recommendations and codes allow using FRP reinforcement in bridge decks and girders as the main reinforcement.

Long-term bridge studies, observations and inspections have been performed and results generated. The results show that deflections, cracking mode and deformations of concrete bridge decks reinforced with FRP

doi:10.3846/bjrbe.2016.03

reinforcement bars are almost the same as those of the decks reinforced with steel reinforcement. It has also been found out that decks reinforced with FRP work very well in an aggressive environment, freeze thaw cycles, sharp temperature fluctuations, de-icing salts, intensive traffic. No additional cracks or their development in concrete constructions have been noticed under such complicated conditions. It has neither been noticed that FRP reinforcement would be damaged by aggressive effects.

FRP reinforcement module is relatively smaller than that of the steel, therefore, it is expected that concrete bending elements reinforced with FRP bars will deflect more than the ones reinforced with steel reinforcement. However, field tests of functioning bridges show that with a proper design of constructions, their deflections do not exceed the permissible ones. Deformability is influenced by the strength of concrete, the height of cross-section, the percentage of reinforcement (Benmokrane *et al.* 2004; Benmokrane *et al.* 2006; El-Ragaby *et al.* 2007).

Bridge decks are exposed to repeated transport loads; therefore, their failure due to fatigue is possible. Bridge decks reinforced with FRP reinforcement bars have a better fatigue performance and a longer fatigue life than the decks reinforced with steel reinforcement bars. This can be explained by the fact that FRP reinforcement and concrete elasticity modules are closer as well as the fact that FRP reinforcement is linear-elastic up to failure.

Designing of bridge decks and load carrying capacity calculations can be done using different design norms. The essence of methods provided in design norms is to solve two balance equations. These equations are a sum of cross-section forces and moments. Ways of calculating the load carrying capacity differ in defining the reinforcement percentage and the failure mode, description of the stress-strain curve of concrete in compression, the ultimate strains of concrete, additional coefficients and calculation assumptions.

2. Analysis of design methods

The research is based on three calculation methods for ultimate moment resistance. These methods are provided in design codes (*fib Bulletin No. 40. FRP Reinforcement in RC Structures* – further in text FIB; *Guide for the Design and Construction of Structural Concrete Reinforced with FRP Bars, ACI 440.1R-06* – further in text ACI; *Reinforcing Concrete Structures with Fibre-Reinforced Polymers. Design Manual No. 3, Version 2, ISIS Canada* – further in text ISIS).

There are a few assumptions on which calculation methods are based:

- sections of an element are plane before and after loading;
- the ultimate compressive strain of concrete ε_{cu} is 0.0035 according to FIB, ISIS and for ACI is equal to 0.003;
- the linear behaviour of FRP reinforcement up to failure;
- the bond between concrete and FRP reinforcement is perfect;
- the tensile concrete performance is ignored.

There are three modes of flexural failure of concrete elements reinforced with FRP. The first is balanced failure when FRP reinforcement ruptures and concrete crushes at the same time. The second is compression failure when concrete crushes before FRP reinforcement reaches its ultimate strain. And the last way of failure is governed by FRP rupture before concrete crushing. According to design codes, the ultimate moment resistance is calculated assessing the failure mode. It is possible to determine the failure mode when the reinforcement ratio ρ_f of FRP reinforcement is compared to the balanced reinforcement ratio ρ_{fb}. The balanced reinforcement ratio is based on the equilibrium of

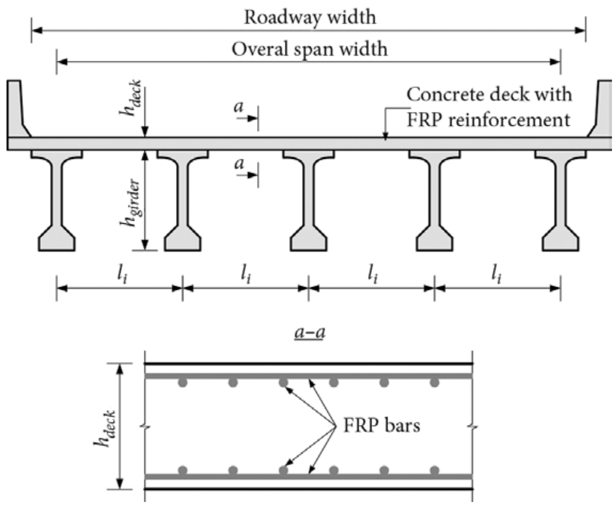

Fig. 1. Bridge cross section

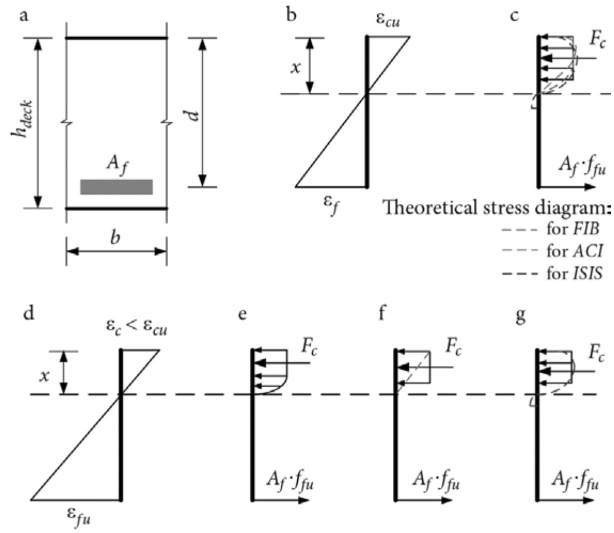

Fig. 2. Design scheme: a – deck cross section; b – strain distribution at compression failure condition; c – design stress distribution at compression failure condition; d – strain distribution at tension failure condition; e – design stress distribution at tension failure condition for FIB, f – for ACI, g – for ISIS

internal forces and can be expressed for FIB as Eq (1), for ACI as Eq (2), for ISIS as Eq (3).

$$\rho_{fb} = \frac{0.81\left(f_{ck}+8\right)\varepsilon_{cu}}{f_{fk}\left(\dfrac{f_{fk}}{E_f}+\varepsilon_{cu}\right)}, \tag{1}$$

$$\rho_{fb} = 0.85\beta_1 \frac{f_c'}{f_{fu}} \frac{E_f \varepsilon_{cu}}{E_f \varepsilon_{cu} + f_{fu}}, \tag{2}$$

$$\rho_{fb} = \alpha_1 \beta_1 \frac{f_c'}{f_{fu}} \left(\frac{\varepsilon_{cu}}{\varepsilon_{cu}+\varepsilon_f}\right), \tag{3}$$

where f_{ck} – the characteristic compressive strength of concrete, MPa; ε_{cu} – ultimate concrete compressive strain; f_{fk} – the characteristic tensile strength of FRP reinforcement, MPa; f_{fu} – the ultimate tensile strength of FRP reinforcement, MPa; E_f – elastic modulus for FRP, MPa; f_c' – the compressive strength of concrete MPa; α_1 and β_1 – stress block factors.

The design scheme is presented in Fig. 1. The flexural concrete element will fail due to concrete crushing if $\rho_f > \rho_{fb}$. When, according to FIB, the ultimate resistance is calculated by equation:

$$M_u = \eta f b_{cd} d^2 \lambda \xi \left(1 - \frac{\lambda \xi}{2}\right), \tag{4}$$

where f_{cd} – the design compressive strength of concrete, MPa; b – the width of the element, m; d – the effective depth of the cross-section, m; η and λ – stress block factors according to Eurocode 2; ξ – ratio of neutral axis depth to the effective depth.

$$\xi = \frac{x}{d} = \frac{\varepsilon_{cu}}{\varepsilon_f + \varepsilon_{cu}}. \tag{5}$$

The strain in FRP reinforcement is calculated:

$$\varepsilon_f = \frac{-\varepsilon_{cu} + \left(\varepsilon_{cu}^2 + \left(\dfrac{4\eta f_{cd} \lambda \varepsilon_{cu}}{\rho_f E_f}\right)\right)^{\frac{1}{2}}}{2}, \tag{6}$$

$$f_f = \varepsilon_f E_f < f_{fd}, \tag{7}$$

where f_f – the stress of FRP reinforcement, MPa; f_{fd} – the design tensile strength of FRP reinforcement, MPa.

According to ACI, the ultimate moment is calculated by Eq (8) when failure of concrete element is initiated by concrete crushing.

$$M_u = \rho_f f_f \left(1 - 0.59 \frac{\rho_f f_f}{f_c'}\right) b d^2, \tag{8}$$

$$f_f = \left(\sqrt{\frac{\left(E_f \varepsilon_{cu}\right)^2}{4} + \frac{0.85\beta_1 f_c'}{\rho_f} E_f \varepsilon_{cu}} - 0.5 E_f \varepsilon_{cu}\right) \le f_{fu}, \tag{9}$$

where f_{fu} – the ultimate stress of FRP reinforcement, MPa.

ISIS presents Eq (10) for ultimate moment calculation when failure is governed by concrete crushing.

$$M_u = \alpha_1 f_c' \beta_1 x b \left(d - \frac{\beta_1 x}{2}\right). \tag{10}$$

The depth of neutral axis is calculated as follows:

$$x = \frac{A_f f_f}{\alpha_1 f_c' \beta_1 b}, \tag{11}$$

$$f_f = 0.5 E_f \varepsilon_{cu} \left(\left(1 + \frac{4\alpha_1 \beta_1 f_c'}{\rho_f E_f \varepsilon_{cu}}\right)^{\frac{1}{2}} - 1\right), \tag{12}$$

where A_f – the cross-sectional area of FRP reinforcement, m^2.

The flexural concrete element will fail due to FRP rupturing if $\rho_f > \rho_{fb}$. At this state calculation of the ultimate moment differs from the one mentioned above because the concrete compressive strain ε_c is unknown.

When calculations are done according to FIB, the ultimate moment is calculated by Eq (13):

$$M_u = A_f f_{fd} d \left(1 - \frac{\xi}{2}\right). \tag{13}$$

The depth of neutral axis is solved by Eqs (14)–(15):

$$\xi = \frac{x}{d} = \frac{\varepsilon_c}{\varepsilon_{fu} + \varepsilon_c}, \tag{14}$$

$$bd\xi \frac{\int_0^{\varepsilon_c} f_c d\varepsilon_c}{\varepsilon_c} = A_f f_{fd}. \tag{15}$$

According to ACI, the calculation of ultimate moment is done in a simplified way when failure is due to FRP rupture:

$$M_u = A_f f_{fd} \left(d - \frac{\beta_1 x}{2}\right), \tag{16}$$

$$x = \frac{\varepsilon_{cu}}{\varepsilon_{fu} + \varepsilon_{cu}} d, \tag{17}$$

where ε_{fu} – the ultimate strain of FRP reinforcement.

According to ISIS, the calculation of the ultimate moment is based on the iteration process Eq (18) to assume the depth of the neutral axis x. The stress block parameters α and β can be found in the tables of code. The ultimate moment is calculated by Eq (19).

$$\alpha f_c' \beta b x = A_f \varepsilon_{fu} E_f. \tag{18}$$

$$M_u = A_f \varepsilon_{fu} E_f \left(d - \frac{\beta x}{2}\right). \tag{19}$$

3. Database and statistical analysis

There were collected 127 experimental results of concrete elements reinforced with FRP bars. Also, a database was created for statistical analysis. All elements included into the database were of rectangular cross-section and tested in four-point bending. No additional preloading or damaging was applied to the elements before tests. The failure modes of tested elements were concrete crushing or FRP reinforcement rupturing.

Table 1 provides the dimensions of the tested elements, properties of materials, experimental ultimate moment M_{exp} and the ratios of experimental and theoretical results $\frac{M_{\text{exp}}}{M_{FIB}}, \frac{M_{\text{exp}}}{M_{ACI}}, \frac{M_{\text{exp}}}{M_{ISIS}}$.

The results of the ultimate moment calculation show that the mean and variation coefficient of the ratio $\frac{M_{\text{exp}}}{M_{i,calc}}$ according to the FIB is 0.95 and 15.6%, according ACI is 1.07 and 14.9%, according ISIS is 1.05 and 14.7%. It is difficult to state the accuracy and relevance of calculation methods from results which are given in Table 1 and Fig. 3.

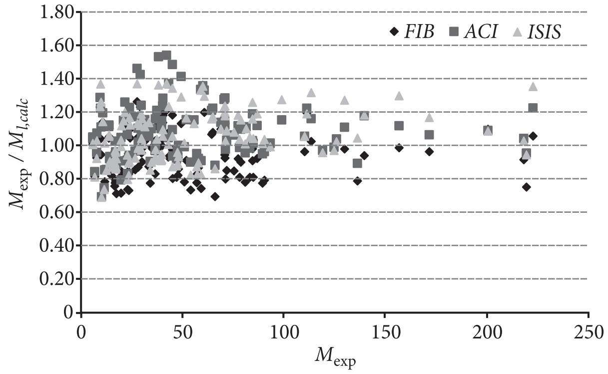

Fig. 3. Results of experimental and calculated ultimate moments

Table 1. Database of concrete elements with FRP reinforcement; results of experimental and calculated ultimate moments

Ref.	No.	Element code	h, mm	b, mm	f_c, MPa	f_{fu}, MPa	E_f, GPa	A_f, mm^2	M_{exp}, kNm	M_{FIB}, kNm	$\frac{M_{\text{exp}}}{M_{FIB}}$	M_{ACI}, kNm	$\frac{M_{\text{exp}}}{M_{ACI}}$	M_{ISIS}, kNm	$\frac{M_{\text{exp}}}{M_{ISIS}}$
1	1	A1	200	150	46.2	1506	50	177	22.8	27.2	0.84	21.5	1.06	24.3	0.94
	2	B1	200	150	46.2	1506	50	265	23.6	32.4	0.73	25.5	0.92	28.8	0.82
	3	C1	200	150	46.2	1506	50	353	28.1	32.4	0.87	25.5	1.10	28.7	0.98
2	4	B	210	200	31	700	36	1134	36.5	44.0	0.83	37.8	0.97	40.1	0.91
	5	C	260	200	31	886	43	507	48.1	56.1	0.86	48.1	1.00	51.6	0.93
	6	D	250	200	41	700	36	1134	54.0	73.8	0.73	60.1	0.90	65.7	0.82
3	7	II	210	200	31.3	700	36	1134	34.2	44.3	0.77	37.9	0.90	40.3	0.85
	8	III	260	200	31.3	886	43	507	45.1	56.4	0.80	48.3	0.93	51.9	0.87
	9	IV	300	200	40.7	700	36	567	59.2	79.9	0.74	65.2	0.91	72.0	0.82
	10	V	250	200	40.7	700	36	1134	57.0	73.5	0.78	60.0	0.95	65.5	0.87
4	11	BG1a	250	150	47.7	665	43	143	17.3	19.8	0.87	19.4	0.89	19.9	0.87
	12	BG1b	250	150	47.7	665	43	143	17.1	19.8	0.87	19.4	0.88	19.9	0.86
	13	BG2a	250	150	47.7	620	42	253	30.9	31.3	0.99	29.0	1.07	30.7	1.01
	14	BG2b	250	150	47.7	620	42	253	29.8	31.3	0.95	29.0	1.03	30.7	0.97
	15	BG3a	250	150	46.5	670	42	1140	43.0	46.3	0.93	41.2	1.04	42.8	1.01
	16	BG3b	250	150	46.5	670	42	1140	45.0	46.3	0.97	41.2	1.09	42.8	1.05
	17	BC1a	250	150	55.4	1450	133	95	28.3	28.4	1.00	27.8	1.02	28.7	0.99
	18	BC1b	250	150	55.4	1450	133	95	29.8	28.4	1.05	27.8	1.07	28.7	1.04
	19	BC3a	250	150	51.8	1475	119	380	47.1	58.3	0.81	51.4	0.92	53.8	0.88
	20	BC3b	250	150	51.8	1475	119	380	47.8	58.3	0.82	51.4	0.93	53.8	0.89
	21	SG1a	120	500	51	600	39	158	7.8	8.4	0.92	8.1	0.96	8.4	0.92
	22	SG1b	120	500	51	600	39	158	6.8	8.4	0.81	8.1	0.84	8.4	0.81
	23	SG2a	120	500	46.2	665	42	357	15.1	18.5	0.82	16.5	0.92	17.4	0.87
	24	SG2b	120	500	46.2	665	42	357	16.9	18.5	0.91	16.5	1.02	17.4	0.97
	25	SG3a	120	500	45.9	670	42	1425	23.5	28.4	0.83	25.3	0.93	26.3	0.89
	26	SG3b	120	500	45.9	670	42	1425	23.8	28.4	0.84	25.3	0.94	26.3	0.90
	27	SC1a	120	500	50.1	1450	133	127	14.3	15.6	0.91	15.3	0.93	15.8	0.90

Continued Table 1

Ref.	No.	Element code	h, mm	b, mm	f_c, MPa	f_{fu}, MPa	E_f, GPa	A_f, mm^2	M_{exp}, kNm	M_{FIB}, kNm	$\frac{M_{exp}}{M_{FIB}}$	M_{ACI}, kNm	$\frac{M_{exp}}{M_{ACI}}$	M_{ISIS}, kNm	$\frac{M_{exp}}{M_{ISIS}}$
4	28	SC1b	120	500	50.1	1450	133	127	14.1	15.6	0.90	15.3	0.92	15.8	0.89
	29	SC3a	120	500	49.8	1475	119	507	23.0	31.3	0.73	27.7	0.83	28.9	0.79
	30	SC3b	120	500	49.8	1475	119	507	26.7	31.3	0.85	27.7	0.96	28.9	0.92
5	31	C1212D1	190	140	32.1	1353	63	226	24.0	21.9	1.09	19.6	1.23	20.6	1.17
	32	C1216D1	190	140	32.5	1015	65	402	29.6	26.9	1.10	23.9	1.24	25.0	1.19
	33	C1316D1	190	140	32.4	1015	65	603	31.4	30.7	1.03	27.3	1.15	28.3	1.11
	34	C1212D2	190	160	32	1353	63	226	21.6	19.3	1.12	17.2	1.26	18.1	1.20
	35	C1216D2	190	160	31.7	1015	65	402	24.2	23.2	1.04	20.7	1.17	21.6	1.12
	36	C1316D2	190	160	31.8	1015	65	603	27.7	26.6	1.04	23.7	1.17	24.6	1.13
	37	C2212D1	190	140	59.8	1353	63	226	38.2	31.7	1.21	25.0	1.53	28.1	1.36
	38	C2216D1	190	140	56.3	1015	65	402	45.1	38.2	1.18	30.4	1.48	33.6	1.34
	39	C2316D1	190	140	55.2	1015	65	603	49.4	43.7	1.13	35.0	1.41	38.3	1.29
	40	C2212D2	190	160	39.6	1353	63	226	27.7	22.0	1.26	19.0	1.46	20.3	1.37
	41	C2216D2	190	160	61.7	1015	65	402	42.2	34.8	1.21	27.4	1.54	30.8	1.37
	42	C2316D2	190	160	60.1	1015	65	603	43.2	40.1	1.08	31.6	1.37	35.1	1.23
6	43	R/C-2	350	200	40.5	1060	200	226	57.3	69.2	0.83	63.1	0.91	69.5	0.83
	44	R/C-4	350	200	40.5	1060	200	452	124.6	126.4	0.99	126.1	0.99	128.7	0.97
7	45	2	200	150	32.56	650	38	57	5.9	5.8	1.01	5.6	1.05	5.8	1.01
	46	4	250	150	32.56	650	38	57	7.9	7.6	1.03	7.3	1.07	7.6	1.03
	47	6	300	150	32.56	650	38	57	10.8	9.5	1.14	9.0	1.19	9.5	1.14
	48	8	200	150	58.93	650	38	57	5.9	5.9	1.00	5.7	1.04	5.9	1.00
	49	10	250	150	58.93	650	38	57	9.5	7.7	1.23	7.4	1.29	7.7	1.23
	50	12	300	150	58.93	650	38	113	16.8	18.8	0.89	18.2	0.92	18.8	0.89
8	51	GB5	250	150	31.2	1000	45	429	40.3	35.5	1.14	32.7	1.23	38.3	1.05
	52	GB9	250	150	39.8	1000	45	429	39.7	39.8	1.00	36.0	1.11	43.5	0.91
	53	GB10	250	150	39.8	1000	45	429	39.5	39.8	0.99	36.0	1.10	43.5	0.91
	54	GB13	250	150	43.4	1000	45	286	34.7	35.3	0.99	31.6	1.10	38.7	0.90
9	55	BGR1.1	180	130	40	647	36	142	13.9	13.2	1.05	12.4	1.12	13.1	1.06
	56	BGR2.1	180	130	40	647	36	142	13.8	13.2	1.04	12.4	1.11	13.1	1.05
	57	BGR3.1	180	130	40	647	36	142	13.8	13.2	1.04	12.4	1.11	13.1	1.05
10	58	CB2B-1	300	200	52	773	38	349	57.9	66.9	0.87	62.9	0.92	64.8	0.89
	59	CB3B1	300	200	52	773	38	523	66.0	95.4	0.69	75.0	0.88	76.8	0.86
	60	CB4B-1	300	200	45	773	38	697	75.4	89.2	0.85	71.1	1.06	69.9	1.08
	61	CB6B-1	300	200	45	773	38	1046	84.8	105.1	0.81	83.7	1.01	81.6	1.04
11	62	C1-4	300	200	40.4	1506	114	284	71.2	89.2	0.80	72.9	0.98	69.6	1.02
	63	C1-6	300	200	39.3	1506	114	426	83.1	102.9	0.81	84.6	0.98	79.4	1.05
	64	C1-8	300	200	39.3	1506	114	568	90.4	114.5	0.79	94.1	0.96	87.4	1.03
	65	C2-4	300	200	39.9	1988	122	256	78.8	87.7	0.90	71.9	1.10	68.4	1.15
	66	C2-4b	300	200	39.9	1988	122	256	78.2	96.8	0.81	79.3	0.99	75.6	1.03
	67	C2-6	300	200	40.8	1988	122	384	80.9	103.9	0.78	84.7	0.95	80.3	1.01
	68	C2-8	300	200	40.8	1988	122	512	89.4	115.7	0.77	94.3	0.95	88.6	1.01
	69	G1-6	300	200	39.05	617	40	774	77.5	84.3	0.92	69.4	1.12	65.7	1.18
	70	G1-8	300	200	39.05	617	40	1032	86.8	94.3	0.92	77.7	1.12	73.0	1.19

Continued Table 1

Ref.	No.	Element code	h, mm	b, mm	f_c, MPa	f_{fu}, MPa	E_f, GPa	A_f, mm^2	$M_{\exp}$, kNm	M_{FIB}, kNm	$\frac{M_{\exp}}{M_{FIB}}$	M_{ACI}, kNm	$\frac{M_{\exp}}{M_{ACI}}$	M_{ISIS}, kNm	$\frac{M_{\exp}}{M_{ISIS}}$
11	71	G2-6	300	200	39.05	747	36	678	71.0	76.9	0.92	63.4	1.12	60.3	1.18
	72	G2-8	300	200	39.05	747	36	904	84.5	86.4	0.98	71.1	1.19	67.3	1.26
	73	AR-6	300	200	39.05	1800	52	426	70.9	75.2	0.94	61.9	1.14	59.1	1.20
	74	AR-8	300	200	39.05	1800	52	568	71.8	84.5	0.85	69.6	1.03	66.0	1.09
12	75	F2	185	500	30	600	42	508	36.8	38.4	0.96	36.6	1.01	37.8	0.97
	76	F3	185	500	30	600	42	889	60.7	50.7	1.20	45.7	1.33	46.9	1.29
13	77	BRC2	200	120	41.71	1676	136	142	29.2	23.8	1.23	20.5	1.42	26.1	1.12
14	78	B4	152.4	152.4	51.73	1900	140	63	12.6	14.7	0.86	14.7	0.85	14.8	0.85
	79	B5	152.4	152.4	48.02	1900	140	63	10.2	14.7	0.69	14.7	0.69	14.8	0.69
	80	B7	152.4	152.4	49.3	1900	140	99	17.1	21.8	0.79	17.8	0.96	17.8	0.96
	81	B8	152.4	152.4	51.1	1900	140	99	16.9	21.9	0.77	18.0	0.94	18.2	0.93
	82	B9	152.4	152.4	53.31	1900	140	99	16.6	21.9	0.76	18.3	0.90	18.5	0.89
	83	B12	152.4	152.4	43.88	1900	140	142	17.5	24.7	0.71	19.8	0.89	19.0	0.92
15	84	GB1-1	300	180	35	695	40	253	60.0	44.1	1.36	44.2	1.36	44.3	1.35
	85	GB1-2	300	180	35	695	40	253	59.0	44.1	1.34	44.2	1.33	44.3	1.33
	86	GB2-1	300	180	35	695	40	380	65.0	60.4	1.08	53.2	1.22	55.5	1.17
	87	GB2-2	300	180	35	695	40	380	64.3	60.4	1.06	53.2	1.21	55.5	1.16
	88	GB3-1	300	180	35	695	40	507	71.0	62.8	1.13	55.3	1.28	57.5	1.23
	89	GB3-2	300	180	35	695	40	507	70.5	62.8	1.12	55.3	1.27	57.5	1.23
16	90	GB1	250	150	30	1000	45	429	37.4	33.5	1.11	30.9	1.21	36.1	1.04
	91	GB5	250	150	31.2	1000	45	429	40.3	34.2	1.18	31.5	1.28	36.9	1.09
	92	GB9	250	150	39.8	1000	45	429	39.7	38.4	1.03	34.7	1.15	42.0	0.95
	93	GB10	250	150	39.8	1000	45	429	39.6	38.4	1.03	34.7	1.14	42.0	0.94
17	94	P4C1	229	179	48	2069	124	219	51.9	57.2	0.91	45.0	1.15	44.6	1.16
	95	P8G1	229	179	48	551	41	1077	50.9	65.3	0.78	51.4	0.99	50.3	1.01
18	96	FB2	400	300	30	690	41	265	68.9	62.9	1.10	60.7	1.14	62.8	1.10
	97	FB3	400	300	30	690	41	398	111.2	93.1	1.19	91.0	1.22	93.5	1.19
	98	FB4	400	300	30	690	41	531	125.9	122.4	1.03	121.3	1.04	123.2	1.02
	99	FB6	400	300	30	690	41	796	171.5	178.4	0.96	161.4	1.06	147.0	1.17
	100	FB8	400	300	30	690	41	1062	222.6	211.1	1.05	182.0	1.22	164.7	1.35
	101	HFB3	400	300	50	690	41	398	93.2	94.2	0.99	92.1	1.01	94.1	0.99
	102	HFB4	400	300	50	690	41	531	119.0	124.4	0.96	122.8	0.97	124.7	0.95
	103	HFB6	400	300	50	690	41	796	200.5	182.9	1.10	184.2	1.09	185.0	1.08
	104	HFB8	400	300	50	690	41	1062	218.0	239.0	0.91	209.6	1.04	212.7	1.03
	105	HFB10	400	300	50	690	41	1327	219.4	292.7	0.75	230.3	0.95	232.7	0.94
19	106	ARD11-2S	120	120	32.64	1389	73	190	9.7	9.3	1.04	7.9	1.22	7.1	1.37
	107	ARD13-2S	120	120	32.64	1299	74	265	9.9	10.5	0.94	8.9	1.11	7.9	1.26
20	108	B1	250	160	48.2	680	38	339	36.7	35.7	1.03	31.7	1.16	39.5	0.93
21	109	B1	200	150	20	700	41	142	11.7	15.0	0.78	13.8	0.85	11.6	1.01
	110	B2	200	150	20	700	41	471	20.0	24.4	0.82	22.0	0.91	17.9	1.12
	111	B3	200	150	20	700	41	671	19.7	27.7	0.71	24.9	0.79	19.9	0.99
	112	B4	200	150	38	700	41	142	11.5	15.6	0.74	15.5	0.74	15.7	0.73
	113	B5	200	150	38	700	41	471	30.1	33.5	0.90	27.7	1.09	26.0	1.16
	114	B6	200	150	38	700	41	671	33.4	38.3	0.87	31.7	1.05	29.4	1.13

Continued Table 1

Ref.	No.	Element code	h, mm	b, mm	f_c, MPa	f_{fu}, MPa	E_f, GPa	A_f, mm^2	M_{exp}, kNm	M_{FIB}, kNm	$\frac{M_{exp}}{M_{FIB}}$	M_{ACI}, kNm	$\frac{M_{exp}}{M_{ACI}}$	M_{ISIS}, kNm	$\frac{M_{exp}}{M_{ISIS}}$
	115	BC2HA	180	130	57.2	773	38	232	19.7	23.3	0.84	18.8	1.05	19.1	1.03
	116	BC4HA	180	130	53.9	773	38	464	21.0	23.0	0.91	18.3	1.15	18.3	1.15
	117	A2D8-27	400	200	25.1	1415	62	100	55.7	49.2	1.13	48.4	1.15	49.4	1.13
	118	A4D8-27	400	200	25.1	1415	62	200	84.5	93.1	0.91	82.2	1.03	73.0	1.16
	119	A6D8-27	412.5	200	25.1	1415	62	300	113.4	110.9	1.02	97.8	1.16	86.2	1.31
	120	A2D8-45	400	200	45.1	1415	62	100	47.6	49.8	0.96	48.9	0.97	49.8	0.96
22	121	A3D8-45	400	200	45.1	1415	62	150	81.4	73.9	1.10	73.3	1.11	74.0	1.10
	122	A3D10-45	400	200	45.1	1415	62	237	110.1	114.5	0.96	104.6	1.05	104.6	1.05
	123	A4D10-45	400	200	45.1	1415	62	316	139.6	148.9	0.94	118.7	1.18	118.2	1.18
	124	C2D8-27	400	200	25.1	2542	143	100	98.9	85.8	1.15	85.9	1.15	77.7	1.27
	125	C4D8-27	400	200	25.1	2542	143	200	129.8	132.9	0.98	117.2	1.11	102.2	1.27
	126	C4D10-27	400	200	25.1	2542	143	316	156.7	159.2	0.98	140.4	1.12	120.9	1.30
	127	C5D10-27	412.5	200	25.1	2542	143	395	136.1	173.2	0.79	152.7	0.89	130.6	1.04
										Mean	0.95		1.07		1.05
										Standard deviation	0.15		0.16		0.15
										Coefficient of variation, %	15.6		14.9		14.7

References: 1 – Aiello, Ombres 2000; 2 – Alsayed *et al.* 1998; 3 – Alsayed *et al.* 2000; 4 – Al-Sunna *et al.* 2012; 5 – Barris *et al.* 2009; 6 – Ashour, Family 2006; 7 – Ashour 2006; 8 – Duranovic *et al.* 1997; 9 – Laoubi *et al.* 2006; 10 – Masmoudi *et al.* 1998; 11 – Kassem *et al.* 2011; 12 – Pecce *et al.* 2000; 13 – Rafi *et al.* 2008; 14 – Thiagarajan 2003; 15 – Toutanji, Deng 2003; 16 – Zhao *et al.* 1997; 17 – Wang, Belarbi 2011; 18 – Shin *et al.* 2009; 19 – Sakurada *et al.* 2006; 20 – Li *et al.* 2012; 21 – Mousavi, Esfahani 2012; 22 – Thériault, Benmokrane 1998; 23 – Lee, Kim 2012.

For this purpose a statistical analysis is performed to assess the accuracy and relevance of the calculation methods. Six data samples were made according to the ratio of FRP reinforcement. The size of samples n, the mean, standard deviations s, *min* and *max* values are provided in Table 2.

Wilk-Shapiro test for a small size sample was applied for determination of the distribution of the sample data (Shapiro, Wilk 1965). The data has normal distribution if the hypothesis is valid:

$$W \geq W_a, \tag{20}$$

where W – Shapiro-Wilk test value calculated according to the Eq (21); W_a – critical value found in tables.

$$W = \frac{\left(\sum_{i=1}^{k} a_{n-i+1} \left(x_{n-i+1} - x_i \right) \right)^2}{\sum_{i=1}^{n} \left(x_i - \overline{x} \right)^2}, \tag{21}$$

where x_i – ratios $\frac{M_{\exp}}{M_{FIB}}, \frac{M_{\exp}}{M_{ACI}}, \frac{M_{\exp}}{M_{ISIS}}$ of the experimental and the theoretical results of the i beam; x – means $\overline{\frac{M_{\exp}}{M_{FIB}}}$, $\overline{\frac{M_{\exp}}{M_{ACI}}}, \overline{\frac{M_{\exp}}{M_{ISIS}}}$ of the ratios of the experimental and the theoretical results; n – the size of the sample; when n is an even number, $k = \frac{n}{2}$; when n is an uneven number, $k = \frac{(n-1)}{2}$; a_{n-i+1} – coefficient taken from tables (Shapiro, Wilk 1965).

Table 2 provides the results of Wilk Shapiro test when the significance level is α = 0.05. The test results show that the hypothesis is valid and all data have normal distribution.

The analysis of the results shows that the calculated and experimental ultimate moments are different. It may be stated that the calculated and theoretical results will be always different but this difference may be statistically negligible (Montgomery, Runger 2002).

The best case is if the means of the ratios $\overline{\frac{M_{\exp}}{M_{i,calc}}}$ equals to 1:

$$\overline{\frac{M_{\exp}}{M_{i,calc}}} = 1. \tag{22}$$

A statistical hypothesis is formed to assess a statistical significance of the Eq (22):

$$\begin{cases} H_0: \ \overline{\frac{M_{\exp}}{M_{i,calc}}} = 1 \\ H_1: \ \overline{\frac{M_{\exp}}{M_{i,calc}}} \neq 1 \end{cases}, \tag{23}$$

where $\overline{\dfrac{M_{\exp}}{M_{i,calc}}}$ are the means of the ratios $\overline{\dfrac{M_{\exp}}{M_{FIB}}}$, $\overline{\dfrac{M_{\exp}}{M_{ACI}}}$, $\overline{\dfrac{M_{\exp}}{M_{ISIS}}}$ of the experimental and theoretical results.

t test can be used when the data has normal distribution. Hypothesis H_0 is rejected and hypothesis H_1 is valid when:

$$|t| > t_{\frac{\alpha}{2,(n-1)}}. \tag{24}$$

Table 2. Sample statistics and results of Shapiro-Wilk test

Sample No.	Sample Size	Element number	ρ_f, %	Variable	Mean	s	min	max	W	W_a	Distribution
1	30	11, 12, 17, 18, 21, 22, 27, 28, 43, 45, 46, 47, 48, 49, 50, 78, 79, 96, 97, 101, 117, 118, 119, 120, 121, 122, 123, 124, 125, 126	0.14–0.44	$\frac{M_{\exp}}{M_{FIB}}$	0.98	0.12	0.69	1.23	0.985	0.927	Normal
				$\frac{M_{\exp}}{M_{ACI}}$	1.03	0.13	0.69	1.29	0.981		Normal
				$\frac{M_{\exp}}{M_{ISIS}}$	1.03	0.16	0.69	1.31	0.971		Normal
2	40	1, 13, 14, 23, 24, 31, 34, 37, 40, 44, 54, 55, 56, 57, 58, 62, 63, 65, 66, 67, 73, 75, 77, 80, 81, 82, 83, 84, 85, 86, 87, 94, 98, 99, 102, 103, 108, 109, 112, 127	0.50–0.99	$\frac{M_{\exp}}{M_{FIB}}$	0.96	0.17	0.71	1.36	0.942	0.94	Normal
				$\frac{M_{\exp}}{M_{ACI}}$	1.08	0.17	0.74	1.53	0.953		Normal
				$\frac{M_{\exp}}{M_{ISIS}}$	1.05	0.14	0.73	1.37	0.948		Normal
3	28	2, 5, 8, 9, 19, 20, 29, 30, 51, 52, 53, 59, 60, 64, 68, 71, 74, 76, 88, 89, 90, 91, 92, 93, 100, 104, 105, 115	1.00–1.45	$\frac{M_{\exp}}{M_{FIB}}$	0.92	0.16	0.69	1.20	0.930	0.924	Normal
				$\frac{M_{\exp}}{M_{ACI}}$	1.06	0.14	0.83	1.33	0.951		Normal
				$\frac{M_{\exp}}{M_{ISIS}}$	1.01	0.15	0.79	1.35	0.940		Normal
4	10	3, 32, 35, 38, 41, 69, 72, 106, 110, 113	1.53–1.94	$\frac{M_{\exp}}{M_{FIB}}$	1.01	0.13	0.82	1.21	0.959	0.842	Normal
				$\frac{M_{\exp}}{M_{ACI}}$	1.20	0.19	0.91	1.54	0.919		Normal
				$\frac{M_{\exp}}{M_{ISIS}}$	1.21	0.13	0.98	1.37	0.932		Normal
5	12	6, 10, 33, 36, 39, 42, 61, 70, 107, 111, 114, 116	2.18–2.87	$\frac{M_{\exp}}{M_{FIB}}$	0.91	0.14	0.71	1.13	0.956	0.859	Normal
				$\frac{M_{\exp}}{M_{ACI}}$	1.10	0.18	0.79	1.41	0.963		Normal
				$\frac{M_{\exp}}{M_{ISIS}}$	1.10	0.15	0.82	1.29	0.929		Normal
6	7	4, 7, 15, 16, 25, 26, 95	3.33–3.93	$\frac{M_{\exp}}{M_{FIB}}$	0.85	0.07	0.77	0.97	0.881	0.803	Normal
				$\frac{M_{\exp}}{M_{ACI}}$	0.98	0.07	0.90	1.09	0.943		Normal
				$\frac{M_{\exp}}{M_{ISIS}}$	0.95	0.08	0.85	1.05	0.910		Normal

If the variance is unknown, t statistics is calculated:

$$t=\frac{\frac{\overline{M_{\exp}}}{M_{calc,i}}-1}{\sqrt{\frac{s^2_{\frac{\exp}{calc,i}}}{n}}}, \tag{25}$$

where $t_{\frac{\alpha}{2,(n-1)}}$ – critical value of the Student's distribution with n–1 degrees of freedom when the significance level is α = 0.05; $s_{\frac{\exp}{i,calc}}$ – the standard deviations $s_{\frac{\exp}{FIB}}$, $s_{\frac{\exp}{ACI}}$, $s_{\frac{\exp}{ISIS}}$ of the ratios of the experimental and the theoretical results.

The confidence interval is calculated:

$$\frac{M_{\exp}}{M_{calc,i}}-t_{\frac{\alpha}{2,n-1}}\frac{s_{\frac{\exp}{calc,i}}}{\sqrt{n}}\leq\frac{\overline{M_{\exp}}}{M_{calc,i}}\leq \frac{\overline{M_{\exp}}}{M_{calc,i}}+t_{\frac{\alpha}{2,n-1}}\frac{s_{\frac{\exp}{calc,i}}}{\sqrt{n}}. \tag{26}$$

Table 3 presents statistical results of testing the hypothesis and confidence intervals when the significance is α = 0.05.

The analysis of statistical results shows that the ratio of experimental and theoretical results only in two samples of six, if calculated according to FIB, statistically significantly differ from the best case when the ratio of results is equal to 1. The differences are statistically negligible in the rest of the samples.

The received statistical results are worse when the ultimate moment is calculated according to ACI. The differences are statistically negligible in three samples. The results of the rest of the samples show that the ratios of the experimental and theoretical results statistically significantly differ from 1.

Also, a half of the results of testing the hypothesis show that the different is statistically significant when calculated according to ISIS.

The received results show that in the first sample the difference is negligible when the ultimate moments are calculated according to all three methods. In samples 5 and 6 the experimental and the theoretical results statistically significantly differ when calculated according to one of the three methods. In samples 2, 3 and 4 the different statistical negligible when calculations are made according to one of the three methods.

It is possible to determine which calculation method is more accurate and whether the difference between the theoretical results is statistically significant when statistics methods are used. For this purpose, a statistical hypothesis is created. Hypothesis H_0 is valid when the means $\frac{\overline{M_{\exp}}}{M_{calc,i}}$ and $\frac{\overline{M_{\exp}}}{M_{calc,i+1}}$ are equal. Alternative hypothesis H_1 is valid then the means are not equal.

$$\begin{cases} H_0: \dfrac{\overline{M_{\exp}}}{M_{calc,i}}=\dfrac{\overline{M_{\exp}}}{M_{calc,i+1}} \\ H_1: \dfrac{\overline{M_{\exp}}}{M_{calc,i}}\neq\dfrac{\overline{M_{\exp}}}{M_{calc,i+1}} \end{cases}. \tag{27}$$

Hypothesis H_0 will be rejected if:

$$|t|>t_{\frac{\alpha}{2,v}}. \tag{28}$$

The degrees of freedom v and t statistic are calculated according to Eqs (28)–(29) when the variances of two samples are unknown and not equal.

$$v=\frac{\left(\frac{s^2_{\frac{\exp}{calc,i}}+s^2_{\frac{\exp}{calc,i+1}}}{n}\right)}{\frac{s^4_{\frac{\exp}{calc,i}}+s^4_{\frac{\exp}{calc,i+1}}}{n^2(n-1)}}. \tag{29}$$

$$t=\frac{\frac{\overline{M_{\exp}}}{M_{calc,i}}-\frac{M_{\exp}}{M_{calc,i+1}}}{\sqrt{\frac{s^2_{\frac{\exp}{calc,i}}+s^2_{\frac{\exp}{calc,i+1}}}{n}}}. \tag{30}$$

Three samples are analyzed and results are given in Tables 4, 5, 6. The analysis of the results shows that the difference between theoretical ultimate moments is statistical negligible in sample 1. There is no statistical difference between theoretical results in sample 6 when calculations of the ultimate moment are done according to ACI and ISIS. However, there is a statistical difference in sample 5 when FIB and ACI methods are used to calculate the ultimate moments.

In order to determine which calculation method is more accurate, it is suggested to calculate the coefficient of confidence (Eq (31)) in data samples 1 and 6 when the differences between theoretical results are statistically negligible (Skuturna, Valivonis 2014b).

$$CC=\frac{1}{\frac{\overline{M_{\exp}}}{M_{calc,i}}\left(1-2CV_{\frac{M_{\exp}}{M_{calc,i}}}\right)}. \tag{31}$$

Table 3. Results of hypothesis testing

Sample number	Variable	Mean	*CV*	*t*	*n*−1	$t_{\frac{\alpha}{2},(n-1)}$	H_0	95% Confidence interval lower	95% Confidence interval higher
1	$\frac{M_{\exp}}{M_{FIB}}$	0.98	12.40	0.867	29	2.045	ACCEPTED	0.94	1.03
	$\frac{M_{\exp}}{M_{ACI}}$	1.03	12.92	1.270	29	2.045	ACCEPTED	0.98	1.08
	$\frac{M_{\exp}}{M_{ISIS}}$	1.03	15.89	1.055	29	2.045	ACCEPTED	0.97	1.09
2	$\frac{M_{\exp}}{M_{FIB}}$	0.96	17.30	1.392	39	2.023	ACCEPTED	0.91	1.02
	$\frac{M_{\exp}}{M_{ACI}}$	1.08	15.88	3.004	39	2.023	REJECTED	1.03	1.14
	$\frac{M_{\exp}}{M_{ISIS}}$	1.05	13.64	2.363	39	2.023	REJECTED	1.01	1.10
3	$\frac{M_{\exp}}{M_{FIB}}$	0.92	16.94	2.781	27	2.052	REJECTED	0.86	0.98
	$\frac{M_{\exp}}{M_{ACI}}$	1.06	13.38	2.354	27	2.052	REJECTED	1.01	1.12
	$\frac{M_{\exp}}{M_{ISIS}}$	1.01	14.60	0.214	27	2.052	ACCEPTED	0.95	1.06
4	$\frac{M_{\exp}}{M_{FIB}}$	1.01	13.20	0.132	9	2.262	ACCEPTED	0.91	1.10
	$\frac{M_{\exp}}{M_{ACI}}$	1.20	15.50	3.467	9	2.262	REJECTED	1.07	1.34
	$\frac{M_{\exp}}{M_{ISIS}}$	1.21	10.43	5.214	9	2.262	REJECTED	1.12	1.30
5	$\frac{M_{\exp}}{M_{FIB}}$	0.91	15.11	2.198	11	2.201	ACCEPTED	0.82	1.00
	$\frac{M_{\exp}}{M_{ACI}}$	1.10	16.18	1.919	11	2.201	ACCEPTED	0.99	1.21
	$\frac{M_{\exp}}{M_{ISIS}}$	1.10	13.31	2.382	11	2.201	REJECTED	1.01	1.19
6	$\frac{M_{\exp}}{M_{FIB}}$	0.85	8.79	5.336	6	2.447	REJECTED	0.78	0.92
	$\frac{M_{\exp}}{M_{ACI}}$	0.98	6.92	0.761	6	2.447	ACCEPTED	0.92	1.04
	$\frac{M_{\exp}}{M_{ISIS}}$	0.95	8.05	1.854	6	2.447	ACCEPTED	0.88	1.02

The coefficient of confidence sets the relation between the means of calculation results and the variation coefficients because it can be complicated to evaluate the design method if they are analyzed separately. The more accurate are the theoretical results of the ultimate moments, the closer they are to the experimental ones if the coefficient of confidence is closer to 1.

The values of the coefficients of confidence in sample 1 for FIB, ACI, ISIS methods are 1.36, 1.31 and 1.42 respectively. In sample 6 the coefficients of confidence for

Table 4. Results of *t* test of sample 1

Sample 1	Statistics		H_0
$\overline{\frac{M_{exp}}{M_{FIB}}} = \overline{\frac{M_{exp}}{M_{ACI}}}$	t	1.522	ACCEPTED
	ν	57.53	
	$t_{\frac{\alpha}{2},\nu}$	2.002	
$\overline{\frac{M_{exp}}{M_{FIB}}} = \overline{\frac{M_{exp}}{M_{ISIS}}}$	t	1.364	ACCEPTED
	ν	53.50	
	$t_{\frac{\alpha}{2},\nu}$	2.006	
$\overline{\frac{M_{exp}}{M_{ACI}}} = \overline{\frac{M_{exp}}{M_{ISIS}}}$	t	0.018	ACCEPTED
	ν	55.66	
	$t_{\frac{\alpha}{2},\nu}$	2.004	

Table 5. Results of *t* test of sample 5

Sample 5	Statistics		H_0
$\overline{\frac{M_{exp}}{M_{FIB}}} = \overline{\frac{M_{exp}}{M_{ACI}}}$	t	2.864	REJECTED
	ν	20.72	
	$t_{\frac{\alpha}{2},\nu}$	2.086	

Table 6. Results of *t* test of sample 6

Sample 6	Statistics		H_0
$\overline{\frac{M_{exp}}{M_{ACI}}} = \overline{\frac{M_{exp}}{M_{ISIS}}}$	t	0.879	ACCEPTED
	ν	11.84	
	$t_{\frac{\alpha}{2},\nu}$	2.201	

ACI and ISIS are very similar to each other: ACI – 1.18, ISIS – 1.26.

4. Conclusions

1. The performed analysis shows that it is complicated to assess the calculation methods only according to the means and variation coefficients of calculation results. Statistical methods such as Wilk-Shapiro, *t* test are proposed to use for assessing the calculation methods of the ultimate moment resistance.

2. According to the experimental results of 127 concrete elements in flexure reinforced with fibre reinforced polymer bars, a statistical research of calculating methods of the ultimate moment was performed.

3. The statistical research has shown that in half of the samples the results significantly differ from the experimental ones when calculations are performed according to *Guide for the Design and Construction of Structural Concrete Reinforced with FRP Bars, ACI 440.1R-06* and *Reinforcing Concrete Structures with Fibre-Reinforced Polymers. Design Manual No. 3, Version 2, ISIS Canada*. Better results can be achieved when calculated according to *fib Bulletin No. 40. FRP Reinforcement in RC Structures*.

4. The research results show that the theoretical results differ statistically insignificantly from each other only in rare samples. When the difference is statistically negligible, it is suggested to calculate the coefficient of confidence to assess the calculation methods. The values of coefficients of confidence show that the results of the ultimate moment resistance are more accurate when calculations are done according to *Guide for the Design and Construction of Structural Concrete Reinforced with FRP Bars, ACI 440.1R-06*.

References

Aiello, M. A.; Ombres, L. 2000. Load-Deflection Analysis of FRP Reinforced Concrete Flexural Members, *Journal of Composites for Construction* 4(4): 164–171. http://dx.doi.org/10.1061/(ASCE)1090-0268(2000)4:4(164)

Aktas, M.; Sumer, Y. 2014. Nonlinear Finite Element Analysis of Damaged and Strengthened Reinforced Concrete Beams, *Journal of Civil Engineering and Management* 20(2): 201–210. http://dx.doi.org/10.3846/13923730.2013.801889

Alsayed, S. H.; Al-Salloum, Y. A.; Almusallam, T. H. 2000. Performance of Glass Fiber Reinforced Plastic Bars as a Reinforcing Material for Concrete Structures, *Composites Part B: Engineering* 31(6–7): 555–567. http://dx.doi.org/10.1016/S1359-8368(99)00049-9

Alsayed, S. H. 1998. Flexural Behaviour of Concrete Beams Reinforced with GFRP Bars, *Cement and Concrete Composites* 20(1): 1–11. http://dx.doi.org/10.1016/S0958-9465(97)00061-9

Al-Sunna, R.; Pilakoutas, K.; Hajirasouliha, I.; Guadagnini, M. 2012. Deflection Behaviour of FRP Reinforced Concrete Beams and Slabs: an Experimental Investigation, *Composites: Part B* 43(5): 2125–2134. http://dx.doi.org/10.1016/j.compositesb.2012.03.007

Ashour, A. F. 2006. Flexural and Shear Capacities of Concrete Beams Reinforced with GFRP Bars, *Construction and Building Materials* 20(10): 1005–1015. http://dx.doi.org/10.1016/j.conbuildmat.2005.06.023

Ashour, A. F.; Family, M. 2006. Tests of Concrete Flanged Beams Reinforced with CFRP Bars, *Magazine of Concrete Research* 58(9): 627–639. http://dx.doi.org/10.1680/macr.2006.58.9.627

Barris, C.; Torres, Ll.; Turon, A.; Baena, M.; Catalan, A. 2009. An Experimental Study of the Flexural Behaviour of GFRP RC Beams and Comparison with Prediction Models, *Composite Structures* 91(3): 286–295. http://dx.doi.org/10.1016/j.compstruct.2009.05.005

Barris, C.; Torres, Ll.; Miàs, C.; Vilanova, I. 2012. Design of FRP Reinforced Concrete Beams for Serviceability Requirements, *Journal of Civil Engineering and Management* 18(6): 843–857. http://dx.doi.org/10.3846/13923730.2012.720934

Benmokrane, B.; El-Salakawy, E.; El-Ragaby, A.; Lackey, T. 2006. Designing and Testing of Concrete Bridge Decks Reinforced with Glass FRP Bars, *Journal of Bridge Engineering* 11(2): 217–229. http://dx.doi.org/10.1061/(ASCE)1084-0702(2006)11:2(217)

Benmokrane, B.; El-Salakawy, E.; Desgagne, G.; Lackey, T. 2004. FRP Bars for Bridges, *Concrete International* 26(8): 84–90.

Benzaid, R.; Mesbah, H. A. 2014. The Confinement of Concrete in Compression Using CFRP Composites – Effective Design Equations, *Journal of Civil Engineering and Management* 20(5): 632–648. http://dx.doi.org/10.3846/13923730.2013.801911

Bouguerra, K.; Ahmed, E. A.; El-Gamal, S.; Benmokrane B. 2011. Testing of Full-Scale Concrete Bridge Deck Slabs Reinforced with Fiber-Reinforced Polymer (FRP) Bars, *Construction and Building Materials* 25: 3956–3965. http://dx.doi.org/10.1016/j.conbuildmat.2011.04.028

Dang, Y.; Xie, N.; Kessel, A.; McVey, E.; Pace, A.; Shi, X. 2014. Accelerated Laboratory Evaluation of Surface Treatments for Protecting Concrete Bridge Decks From Salt Scaling, *Construction and Building Materials* 55: 128–135. http://dx.doi.org/10.1016/j.conbuildmat.2014.01.014

Daugevičius, M.; Valivonis, J.; Marčiukaitis, G. 2012. Deflection Analysis of Reinforced Concrete Beams Strengthened with Carbon Fibre Reinforced Polymer under Long-Term Load Action, *Journal of Zhejiang University-Science* 13(8): 571–583. http://dx.doi.org/10.1631/jzus.A1100317

Duranovic, N.; Pilakoutas, K.; Waldron, P. 1997. Tests on Concrete Beams Reinforced with Glass Fibre Reinforced Plastic Bars, in *Proc. of the 3rd International Symposium on Non-Metalic (FRP) Reinforcement for Concrete Structures*, vol. 2. 14–16 October 1997, Sapporo, Japan. Japan Concrete Institute, 1997, 479–486.

El-Ragaby, A.; El-Salakawy, E.; Benmokrane, B. 2007. Fatigue Analysis of Concrete Bridge Deck Slabs Reinforced with E-Glass/Vinyl Ester FRP Reinforcing Bars, *Composites Part B: Engineering* 5–6: 703–711. http://dx.doi.org/10.1016/j.compositesb.2006.07.012

Fayyadh, M. M.; Razak, H. A. 2014. Analytical and Experimental Study on Repair Effectiveness of CFRP Sheets for RC Beams, *Journal of Civil Engineering and Management* 20(1): 21–31. http://dx.doi.org/10.3846/13923730.2013.799095

Hassan, T.; Abdelrahman, A.; Tadros, G.; Rizkalla, S. 2000. Fibre Reinforced Polymer Reinforcing Bars for Bridge Decks, *Canadian Journal of Civil Engineering* 27(5): 839–849. http://dx.doi.org/10.1139/l99-098

Kassem, C.; Farghaly, A.; Benmokrane, B. 2011. Evaluation of Flexural Behavior and Serviceability Performance of Concrete Beams Reinforced with FRP Bars, *Journal of Composites for Construction* 15(5): 682–695. http://dx.doi.org/10.1061/(ASCE)CC.1943-5614.0000216

Lale Arefi, S.; Naghipour, M.; Turskis, Z.; Nematzadeh, M. 2014. Evaluation of Grooving Method to Postpone Debonding of FRP Laminates in WPC-FRP Beams, *Journal of Civil Engineering and Management* 20(2): 237–246. http://dx.doi.org/10.3846/13923730.2013.878379

Laoubi, K.; El-Salakawy, E.; Benmokrane, B. 2006. Creep and Durability of Sand-Coated Glass FRP Bars in Concrete Elements under Freeze/Thaw Cycling and Sustained Loads, *Cement and Concrete Composites* 28(10): 869–878. http://dx.doi.org/10.1016/j.cemconcomp.2006.07.014

Lapko, A.; Urbanski, M. 2015. Experimental and Theoretical Analysis of Deflections of Concrete Beams Reinforced with Basalt Rebar, *Archives of Civil and Mechanical Engineering* 15(1): 223–230. http://dx.doi.org/10.1016/j.acme.2014.03.008

Lee, Y. H.; Kim, M. S. 2012. Flexural Behavior and Deflection Prediction of Concrete Beams Reinforced with AFRP and CFRP Bars, *Special Publication* 284: 1–26.

Li, X.; Lv, H.; Zhou, S. 2012. Flexural Behavior of GFRP-Reinforced Concrete Encased Steel Composite Beams, *Construction and Building Materials* 28(1): 255–262. http://dx.doi.org/10.1016/j.conbuildmat.2011.08.058

Marčiukaitis, G.; Valivonis, J.; Bareišis, J. 2007. An Analysis of the Joint Operation of a CFRP Concrete in Flexural Elements, *Mechanics of Composite Materials* 43(5): 467–478. http://dx.doi.org/10.1007/s11029-007-0044-9

Masmoudi, R.; Thériault, M.; Benmokrane, B. 1998. Flexural Behavior of Concrete Beams Reinforced with Deformed Fiber Reinforced Plastic Reinforcing Rods, *ACI Structural Journal* 95(6): 665–676.

Matta, F.; Nanni, A. 2009. Connection of Concrete Railing Post and Bridge Deck with Internal FRP Reinforcement, *Journal of Bridge Engineering* 14(1): 66–76. http://dx.doi.org/10.1061/(ASCE)1084-0702(2009)14:1(66)

Meisami, M. H.; Mostofinejad, D.; Nakamura, H. 2013. Punching Shear Strengthening of Two-Way Flat Slabs Using CFRP Rods, *Composite Structures* 99: 112–122. http://dx.doi.org/10.1016/j.compstruct.2012.11.028

Montgomery, D. C.; Runger, G. C. 2002. *Applied Statistics and Probability for Engineers*. 3rd ed. John Wiley & Sons. 822 p.

Mostofinejad, D.; Ilia, E. 2014. Confining of Square RC Columns with FRP Sheets Using Corner Strip–Batten Technique, *Construction and Building Materials* 70: 269–278. http://dx.doi.org/10.1016/j.conbuildmat.2014.07.073

Mostofinejad, D.; Moghaddas, A. 2014. Bond Efficiency of EBR and EBROG Methods in Different Flexural Failure Mechanisms of FRP Strengthened RC Beams, *Construction and Building Materials* 54: 605–614. http://dx.doi.org/10.1016/j.conbuildmat.2014.01.002

Mousavi, S. R.; Esfahani, M. R. 2012. Effective Moment of Inertia Prediction of FRP-Reinforced Concrete Beams Based on Experimental Results, *Journal of Composites for Construction* 16(5): 490–498. http://dx.doi.org/10.1061/(ASCE)CC.1943-5614.0000284

Nelson, M.; Fam, A. 2014. Full Bridge Testing at Scale Constructed with Novel FRP Stay-in-Place Structural Forms for Concrete Deck, *Construction and Building Materials* 50: 368–376. http://dx.doi.org/10.1016/j.conbuildmat.2013.09.056

Pakrastinsh, L.; Rocens, K.; Serdjuks, D. 2006. Deformability of Hierarchic Cable Roof, *Journal of Constructional Steel Research* 62(12): 1295–1301. http://dx.doi.org/10.1016/j.jcsr.2006.04.025

Pecce, M.; Manfredi, G.; Cosenza, E. 2000. Experimental Response and Code Models of GFRP RC Beams in Bending, *Journal of Composites for Construction* 4(4): 182–190. http://dx.doi.org/10.1061/(ASCE)1090-0268(2000)4:4(182)

Rafi, M. M.; Ali Nadjai, A. N.; Ali, F.; Talamona, D. 2008. Aspects of Behaviour of CFRP Reinforced Concrete Beams in Bending, *Construction and Building Materials* 22(3): 277–285. http://dx.doi.org/10.1016/j.conbuildmat.2006.08.014

Sakurada, R.; Shimomura, T.; Maruyama, K.; Matsubara, S. 2006. Bending Behavior of RC Beam Reinforced with Braided Aramid FRP Bar, in *Proc. of the 31st Conference on Our World in Concrete & Structures*, 16–17 August 2006, Singapore. Available from Internet: http://www.cipremier.com/e107_files/downloads/Papers/100/31/100031043.pdf

Serdjuks, D.; Rocens, K.; Pakrastinsh, L. 2003. Prestress Losses in the Stabilizing Cables of a Composite Saddle-Shaped Cable Roof, *Mechanics of Composite Materials* 39(4): 341–346. http://dx.doi.org/10.1023/A:1025646612012

Shapiro, S. S.; Wilk, M. B. 1965. An Analysis of Variance Test for Normality, *Biometrika* 52(3-4): 591–611. http://dx.doi.org/10.2307/2333709

Shin, S.; Seo, D.; Han, B. 2009. Performance of Concrete Beams Reinforced with GFRP Bars, *Journal of Asian Architecture and Building Engineering* 8(1): 197–204. http://dx.doi.org/10.3130/jaabe.8.197

Skuturna, T.; Valivonis, J. 2014 a. Design Method for Calculating Load-Carrying Capacity of Reinforced Concrete Beams Strengthened with External FRP, *Construction and Building Materials* 50: 577–583. http://dx.doi.org/10.1016/j.conbuildmat.2013.10.015

Skuturna, T.; Valivonis, J. 2014b. The Statistical Evaluation of Design Methods of the Load-Carrying Capacity of Flexural Reinforced Concrete Elements Strengthened with FRP, *Archives of Civil and Mechanical Engineering* 15(1): 214–222. http://dx.doi.org/10.1016/j.acme.2014.04.005

Sprince, A.; Korjakins, A.; Pakrastinsh, L. 2013. Time-Dependent Behavior of High Performance Fiber-Reinforced Concrete, *Advanced Materials Research* 705: 75–80. http://dx.doi.org/10.4028/www.scientific.net/AMR.705.75

Sundarraja, M. C.; Prabhu, G. G. 2013. Behaviour of CFST Members under Compression Externally Reinforced by CFRP Composites, *Journal of Civil Engineering and Management* 19(2): 184–195. http://dx.doi.org/10.3846/13923730.2012.743925

Szolomicki, J.; Berkowski, P.; Baranski, J. 2015. Computer Modelling of Masonry Cross Vaults Strengthened with Fiber Reinforced Polymer Strips, *Archives of Civil and Mechanical Engineering* 15(3): 751–766. http://dx.doi.org/10.1016/j.acme.2014.05.006

Thériault, M.; Benmokrane, B. 1998. Effects of FRP Reinforcement Ratio and Concrete Strength on Flexural Behavior of Concrete Beams, *Journal of Composites for Construction* 2(1): 7–16. http://dx.doi.org/10.1061/(ASCE)1090-0268(1998)2:1(7)

Thiagarajan, G. 2003. Experimental and Analytical Behavior of Carbon Fiber-Based Rods as Flexural Reinforcement, *Journal of Composites for Construction* 7(1): 64–72. http://dx.doi.org/10.1061/(ASCE)1090-0268(2003)7:1(64)

Toutanji, H.; Deng, Y. 2003. Deflection and Crack-Width Prediction of Concrete Beams Reinforced with Glass FRP Rods, *Construction and Building Materials* 17(1): 69–74. http://dx.doi.org/10.1016/S0950-0618(02)00094-6

Valivonis, J.; Jonaitis, B.; Zavalis, R.; Skuturna, T.; Šneideris, A. 2014. Flexural Capacity and Stiffness of Monolithic Biaxial Hollow Slabs, *Journal of Civil Engineering and Management* 20(5): 693–701. http://dx.doi.org/10.3846/13923730.2014.917122

Wang, H.; Belarbi, A. 2011. Ductility Characteristics of Fiber-Reinforced-Concrete Beams Reinforced with FRP Rebars, *Construction and Building Materials* 25(5): 2391–2401. http://dx.doi.org/10.1016/j.conbuildmat.2010.11.040

Zhao, W.; Pilakoutas, K.; Waldron, P. 1997. FRP Reinforced Concrete: Cracking Behaviour and Determination, in *Proc. of the 3rd International Symposium on Non-Metalic (FRP) Reinforcement for Concrete Structures*, vol. 2, 14–16 October 1997, Sapporo, Japan. Japan Concrete Institute, 439–446.

Received 2 April 2014; accepted 29 May 2014